Local Stress Relaxation and Shear-banding in a Dry Foam under Shear

Alexandre Kabla and Georges Debrégeas*

LFO - Collège de France, CNRS UMR 7125, Paris, France

(Dated: July 1, 2003)

We have developed a realistic simulation of 2D dry foams under quasi-static shear. After a short transient, a shear-banding instability is observed. These results are compared with measurements obtained on real 2D (confined) foams. The numerical model allows us to exhibit the mechanical response of the material to a single plastication event. From the analysis of this elastic propagator, we propose a scenario for the onset and stability of the flow localization process in foams, which should remain valid for most athermal amorphous systems under creep flow.

PACS numbers: 05.40.-a 83.50.-v 83.60.-a

Amorphous glassy materials are ubiquitous in industry and nature: they include silica-based glass-formers and polymer melts below T_g, dense colloidal suspensions and emulsions, foams and dense granular systems. Unlike crystalline solids, plasticity in such systems originates from discrete *local* relaxation events [1, 2], involving a small number of particles (atoms, grains, bubbles, etc...). Spatial and time correlations in the occurrence of these plastic events are generally important, leading to avalanche-like dynamics [3, 4, 5] and spatially inhomogeneous flows [6, 7, 8]. Glassy rheology thus remains one of the most active and challenging domains of statistical physics.

Amongst the large number of theoretical and numerical models recently proposed, foam has emerged as a strongly inspiring model system [9, 10, 11]. First, because thermal energy is strictly irrelevant on bubble scale, creep flow experiments can be run (by imposing an infinitely low deformation rate) in which time dependent effects are absent. Second, the bubble mechanics is simple and yields a wide linear elastic regime. Finally, plasticity in foams is associated with well identified processes. In spite of this apparent simplicity, many features of foams flow remain to date unexplained [12]. Thus, shear-banding flows have been recently exhibited in a 2D Couette experiment [13]. In this study, a monolayer of bubbles squeezed between two glass plates was slowly sheared between two concentric discs. Much of the rearrangements were found to occur in a thin region (a few bubbles in width) along the edge of the inner disc. In the present letter, we directly address this question by developing a numerical model adapted to the quasi-static shearing of 2D dry foams. The observed flow features are compared with experimental data obtained with the same set-up as in [13]. This model allows us to investigate the micro-scale mechanics of the foam leading to strain localization.

We use Voronoi tessalation to build polydisperse structures of $W \times L = 16 \times 48$ cells separated by straight segments. These are later referred as bubbles and films respectively, by analogy with real foams, the intercept between films being called a vertex. These structures
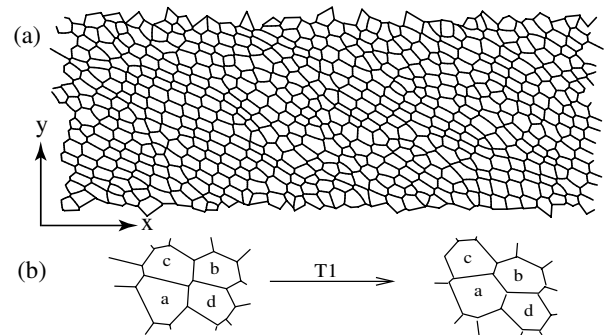

FIG. 1: (a) Snapshot of a simulated foam with 16×48 bubbles. The polydispersity is 6%. The foam has periodic boundary conditions along the x direction. Films laying at upper and lower edges are fixed; shearing is obtained by moving the lower edge along the x direction. (b) Example of a topological change ($T1$ process) occurring inside the foam upon shearing.

have periodic boundary conditions along the x direction, and films laying at the upper and lower edges are fixed to allow subsequent plane parallel shearing (Fig. 1(a)). To obtain a mechanically equilibrated structure, the total film length is minimized at fixed topology and with a constant volume constraint on each bubble, as expected for static dry foams [14]. Our algorithm is based on Surface Evolver [15], a software widely used in foams structural studies [16]. The main difficulty of this minimization procedure comes from the existence of very soft modes associated with large-scale shear deformations [17]. A special care is thus put in equilibrating these modes. The overall procedure is then validated by imposing various strain fields to the initial foam, and checking that the resulting equilibrated structure remains unchanged.

Once the foam has been mechanically equilibrated, plasticity is introduced by allowing $T1$ rearrangements - the elementary topological changes in 2D foams (see Fig. 1(b)). In a real dry foam, vertices have a finite size which depends on the liquid fraction. When a film becomes smaller than this length, the two vertices attract and a $T1$ event is triggered. We mimic this criterion by exchanging bubbles neighbors when one of the film

length falls below a fixed value l_v, corresponding to a liquid fraction $\phi = 1\%$. The $T1$ events are triggered one at a time and followed by a complete mechanical equilibration. This two-step procedure is iterated until all films are stable with regards to the $T1$ criterion. It should be noted that this procedure might not precisely reflect the physical process taking place during an avalanche of $T1$ events. Indeed, in a real foam plasticity and mechanical equilibration take place simultaneously. Our procedure implicitly assumes the latter to be much faster than the $T1$ event. Finally, the foam is quasi-statically sheared by iteratively moving the lower edge over a short distance then equilibrating the structure and allowing plastic events.
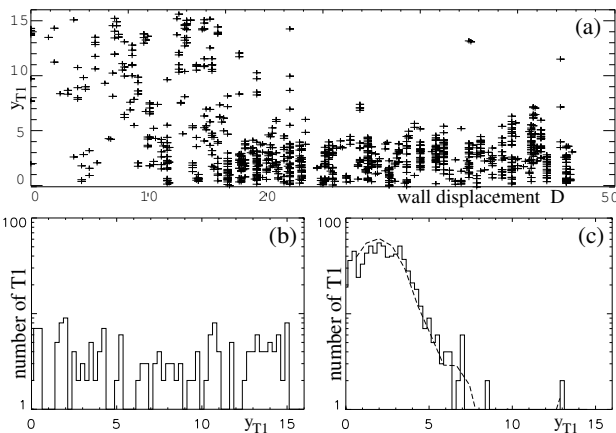

FIG. 2: Localization process in a simulated foam. (a) The $y-$position of the $T1$ events as a function of the wall displacement D expressed in bubble diameter. (b) Distribution of the $y-$positions of the $T1$ events for $D < 15$ (transient regime) and (c) $D > 20$ (localized regime). In the latter, the dotted line shows the gradient $\frac{\partial \overline{v}}{\partial y}(y)$ of the associated plastic flow profile $\overline{v}(y)$.

Figure 2 conveys the main result of the present study: it displays the y_{T1} positions of the rearrangements as a function of the imposed wall displacement D. After a short transient (for $D \sim W$ $i.e.$ an imposed strain ~ 1), the rearrangements permanently gather within a thin shear-band in the vicinity of the lower wall. This strain instability is observed for all the simulations, with a flow localization taking place on either wall depending on the initial foam structure. In the following we mainly focus on measurements performed in the steady-state localized regime.

From the sequence of equilibrated structures, we measure the trajectories of the bubbles centers to extract the flow field at each time step. Furthermore, we can compute the internal shear stress on any sub-volume w using the following relation (where the summation is performed over all segments $\vec{l}$ inside w) [12]:

$$\sigma_{xy}(w) = \frac{1}{w} \cdot \sum_{\vec{l} \in w} \frac{l_x \cdot l_y}{l} \tag{1}$$

We have compared time averaged measurements from the simulation with experimental data we obtained using the same liquid fraction ($\phi = 1\%$). Figure 3 shows the tangential velocity profiles and the normal velocity fluctuations for the experiment and the simulation. For both quantities, we observe similar decays with the distance from the wall. Other flow features, such as the stress fluctuations profiles (presented below), show a similarly good agreement. This adequacy proves the validity of the present simulation. Conversely, it demonstrates that the shear-banding observed in [13] is not due to the Couette geometry, in which the mean stress decreases with the distance from the inner disc.
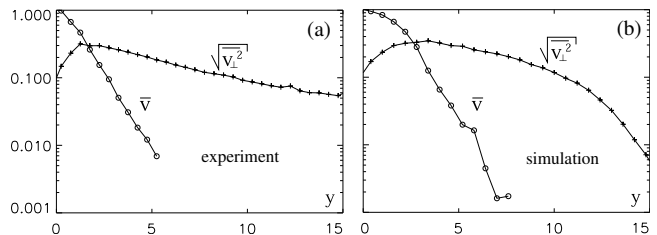

FIG. 3: comparison of time averaged measurements obtained from (a) experiments on 2D foams in a Couette cell (b) simulated foams. $\overline{v}$ is the tangential velocity rescaled by the wall velocity v_0. $\sqrt{\overline{v_\perp^2}}$ is the normal mean square displacement, associated with a time-lapse $\tau = 0.25$ d/v_0, where d is the average bubble diameter. The rapid drop of $\sqrt{\overline{v_\perp^2}}$ in (b) far from the moving wall is due to the relatively small width of the simulated foam ($W = 16$), and hence the presence of the other confining wall.

Beyond these time averaged measurements, the simulation allows one to study the evolution of the foam on short time scales. The dynamics can be separated into two elementary processes, associated with different simulation time steps: (i) charge periods over which the position of the wall is incremented without plastication. The resulting deformation is linear and the shear stress tensor uniformly increases. This allows us to extract a shear elastic modulus μ. This modulus is found to weakly depend on the total applied strain and is considered as a constant in the following. (ii) plastic yielding, during which the stress is relaxed through discrete $T1$ events. To analyze in detail the latter, we focus on the displacement and shear stress fluctuation fields produced by a single rearrangement. The spatial resolution is enhanced to below one bubble diameter by averaging these results over 100 individual $T1$ events located at the same y_{T1} coordinate.
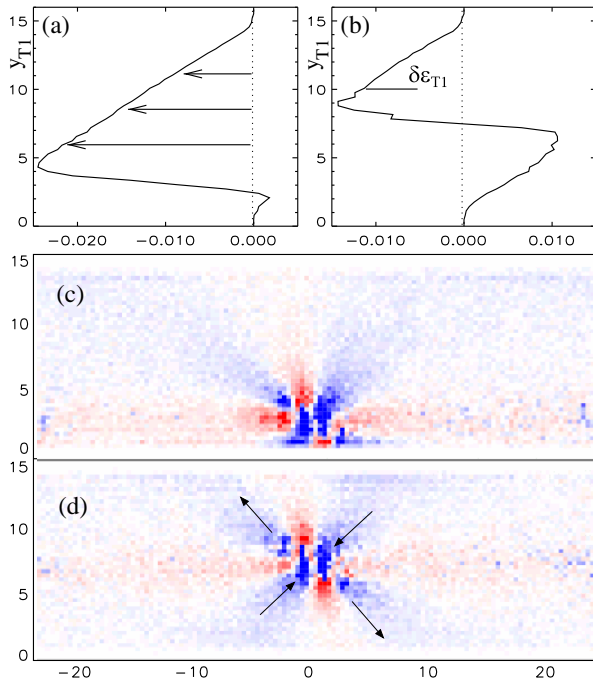
FIG. 4: Displacement and variational shear stress field associated with a single $T1$ event. Each of these results have been obtained by averaging over ~ 100 different $T1$ events located at the same distance y_{T1} from the shearing wall. (a) and (b): line averaged displacement profiles (expressed in bubble diameter d), for a $T1$ event located at $y_{T1} = 3$ and 8 respectively. $\delta\epsilon_{T1}$ represents the mean strain released by the $T1$ event. (c) and (d): Corresponding shear stress variation fields. Red color indicates an increase of the stress (relative to the imposed shear stress), blue color indicates a stress relaxation. The arrows show approximately the motion of the rearranging bubbles during the $T1$ event.

Figure 4 (a) and (b) display the average displacement profiles associated with $T1$ events located at two different distances y_{T1} from the lower wall. Both profiles exhibit a strong discontinuity at the rearranging line whereas the rest of the material is uniformly deformed with a strain amplitude $\delta\epsilon_{T1}$. Regardless of the position y_{T1}, $\delta\epsilon_{T1} = 1.07\, d^2/(WL)$ (with a 30% statistical dispersion over different $T1$ events), where d is the mean bubble diameter and WL is the foam area.

This elementary strain $\delta\epsilon_{T_1}$ can be interpreted from two different viewpoints. On one hand, it represents a *plastic* strain amplitude: each $T1$ event increments the plastic flow gradient at $y = y_{T1}$ by $-\delta\epsilon_{T1}$ in average. This yields the following kinematic relation between the plastic flow profile $\overline{v}(y)$ and the spatial distribution of $T1$ events:

$$\frac{\partial \overline{v}}{\partial y}(y) = -W\,\omega(y)\,\delta\epsilon_{T_1} \qquad (2)$$

where $\omega(y)dy$ is the frequency of $T1$ events occurring between y and $y + dy$. This relation can be directly exhibited by over-plotting the plastic velocity gradient on the $T1$ spatial distributions (see Fig. 2(c)). On the other hand, $\delta\epsilon_{T_1}$ is a uniform elastic strain relaxation. The associated stress can be independently evaluated using Eq. (3) yielding a line-averaged uniform stress release $\delta\sigma_{T1} = \mu\delta\epsilon_{T1}$. By taking into account both the elastic charge and $T1$ relaxation, we derive an equation of evolution of the line-averaged shear stress $\overline{\sigma}(y)$, valid for any line y between 0 and W:

$$\mu\dot{\gamma} - \mu\delta\epsilon_{T1}\int_0^W \omega(y')dy' = \frac{\partial\overline{\sigma}(y)}{\partial t} = 0 \qquad (3)$$

The first term of the left-hand side of the equation corresponds to the advective charge induced by the imposed shear at strain rate $\dot{\gamma}$. The second term comes from the cumulative relaxation of stress associated with the $T1$ processes. The integral form of this equation is a direct consequence of the long range mechanical relaxation associated with each $T1$ process. As a result, this line-averaged mechanical analysis can not allow one to predict a flow profile, and is in fact strictly equivalent to Eq. (2) from which it can be deduced by simple integration. In other words, any velocity profile which obeys the kinematic boundary conditions is mechanically admissible.

The understanding of the shear-banding instability finally comes down to the following question: All lines bearing in average the same stress, why are $T1$ events unevenly distributed amongst them? To capture this process, we need to go beyond the line-averaged analysis and examine the spatial structure of stress release associated with individual T1 events. This is shown in Fig. 4 (c) and (d), for two different y_{T1} locations. As it appears clearly, the stress release is very inhomogeneous and anisotropic, owing to the systematic displacement pattern of the rearranging bubbles imposed by the shearing [8, 18]. In particular, lines in the vicinity of the rearranging site experience large stress modifications. Although the global effect is a release of the main shear stress, some regions (which appear in red) get over-charged. By contrast, remote lines are homogeneously relaxed.

From this measurement, one may expect that T1 events do not only relax the global stress but also cumulatively modify the statistical properties of the frozen stress field. To investigate this effect, we measure the shear stress distributions $P(\sigma(x,y))$ at different distances y from the shearing wall. We extract from these distributions the local variances $\Delta\sigma^2(y) = \langle(\sigma(x,y) - \overline{\sigma})^2\rangle$. We then compare these profiles obtained from foam structures before shearing and after full localization. As shown in Fig. 5, the shearing induces an inhomogeneous modification of these profiles: a large increase of $\Delta\sigma^2$ occurs

in the shear band region where many T1 events have oc-
curred, in both the experiment and the simulation. By
contrast, the stress distributions in lines away from the
shear band display no modification, or even a small de-
crease of their variance. The latter is due to T1's occur-
ring during the transient period of charge which do not
have a systematic orientation. We therefore postpone the
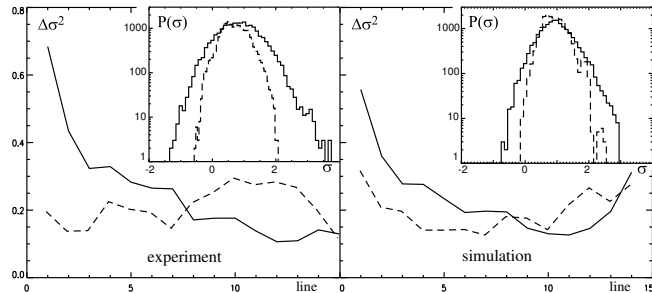discussion of this effect.

FIG. 5: Profile of shear stress variance $\langle(\sigma(x,y)-\overline{\sigma})^2\rangle$ in real
(left) and simulated (right) foams. Solid lines correspond to
foams in the fully localized regime. Dashed lines correspond
to freshly prepared samples (no shearing). All data have been
rescaled with the long time limit shear stress. Inset : shear
stress probability distributions at lines $y = 1$ (solid) and $y =
10$ (dashed) respectively, in the localized regime.

This result shows that the strain history of the foam
is permanently imprinted in its frozen stress field, and
that such modification can be directly probed through
measurements of $\Delta\sigma^2$. This parameter has a further im-
portant physical meaning: large values of $\Delta\sigma^2$ indicate
that a large fraction of bubbles are highly deformed and
therefore more likely to rearrange upon increasing the
global stress. This parameter thus provides a local mea-
surement of the foam "fragility".

Based on these observations, a simple scenario for
strain localization in quasi-static shearing can be
proposed. Starting with a homogeneous structure,
shear-banding develops through a self-amplification
process: $T1$ events locally weaken the foam structure
by increasing its frozen stress disorder. This in turn
enhances the probability for subsequent rearrangements
to take place in neighboring lines. This mechanism
spontaneously leads to the formation of a single shear-
band in the material. Within this scheme, we can also
qualitatively understand why shear-bands preferentially
develop along the boundaries, even in plane parallel
shearing geometry where the average shear stress is
uniform. Indeed, the presence of a rigid boundary with a
no-slip condition imposes an extra mechanical constraint
to the foam in the vicinity of the walls. This tends to
locally enlarge the local stress distributions.

The experimental and numerical systems studied here
provides an ideal model to study plasticity in disordered

media. It allowed us to access detailed mechanical fea-
tures, from the stress signature associated with a sin-
gle plastic event, to the statistical modifications of the
frozen stress field associated with a fully developed shear
flow. We have used these results to propose a simple sce-
nario for shear localization based on a strain weakening
process. Most results obtained with this model system
should remain valid to any material provided the exis-
tence of (i) frozen disorder (no thermal relaxation), (ii)
elastic behavior at low deformation, (iii) local discrete
plastication processes. It could therefore serve as a useful
test to more elaborated models of plasticity that involve
local stress relaxations [1, 8, 19] but do not necessarily
address foam rheology.

* Electronic address: georges.debregeas@college-de-france.fr
[1] V.V. Bulatov and A.S. Argon, Modell. Simul. Mater. Sci.
Eng. **2**, 167 (1994).
[2] M.L. Falk and J.S. Langer, Phys. Rev. E **57**, 7192 (1998).
[3] Kan Chen, Per Bak and S.P. Obukhov, Phys. Rev. A
43, 625-630 (1991).
[4] Y. Jiang , P.J. Swart , A. Saxena , M. Asipauskas and
J.A. Glazier, Phys. Rev. E **59**, 5819 (1999).
[5] S. Tewari , D. Schiemann , D.J. Durian , C.M. Knobler ,
S.A. Langer and A.J. Liu, Phys. Rev. E **60**, 4385 (1999).
[6] P. Hébraud , F. Lequeux, J.P. Munch and D.J. Pine,
Phys. Rev. Lett. **78**, 4657 (1997).
[7] D. Mueth , G. Debrégeas, G. Karczmar, P.J. Eng, S.
Nagel and H. Jaeger, Nature (London) **406**, 385 (2001).
[8] J.S. Langer, Phys. Rev. E **64**, 11504 (2001).
[9] P. Sollich , F. Lequeux, P. Hébraud and M.E. Cates,
Phys. Rev. Lett. **78**, 2020 (1997).
[10] D.J. Durian, Phys. Rev. E **55**, 1739 (1997).
[11] I.K. Ono , C.S. O'Hern, D.J. Durian, S.A. Langer, A.J.
Liu and S.R. Nagel, Phys. Rev. Lett. **89**, 095703 (2002).
[12] D. Weaire and S. Hutzler, *The Physics of Foams*, Claren-
don Press, Oxford, 1999.
[13] G. Debrégeas , H. Tabuteau and J.M. di Meglio, Phys.
Rev. Lett. **87**, 178305 (2001).
[14] D. Weaire and J.P. Kermode, Phil. Mag. B **50**, 379
(1983).
[15] K. Brakke, Experimental mathematics **1**, 141-165 (1992)
[16] D.A. Reinelt and A.M. Kraynik, J. Rheol. **44**, 453 (2000).
[17] T. Herdtle and H. Aref, J. Fluid Mech. **241**, 233 (1992).
[18] We were actually able to reproduce this propagator using
a finite element algorithm (CASTEM2000), by imposing
a quadrupolar displacement in a 2D incompressible elas-
tic medium, with identical boundary conditions. This in-
dicates that beyond the rearranging bubbles, the foam
responds as an elastic body to the plastication event.
[19] C. Derec , A. Ajdari and F. Lequeux, Eur. Phys. J. **4**,
355-361 (2001).